Electron Impact Ionization of Air Molecules and Its Application to the Abatement of Volatile Organic Compounds

B. M. Penetrante, M. C. Hsiao, J. N. Bardsley
B. T. Merritt, G. E. Vogtlin, P. H. Wallman
Lawrence Livermore National Laboratory, Livermore, CA

A. Kuthi, C. P. Burkhart, J. R. Bayless
First Point Scientific, Inc., Agoura Hills, CA

ELECTRON-IMPACT IONIZATION OF AIR MOLECULES AND ITS APPLICATION TO THE ABATEMENT OF VOLATILE ORGANIC COMPOUNDS

B. M. Penetrante, M. C. Hsiao, J. N. Bardsley,
B. T. Merritt, G. E. Vogtlin and P. H. Wallman
Lawrence Livermore National Laboratory, Livermore, California 94550

A. Kuthi, C. P. Burkhart and J. R. Bayless
First Point Scientific, Inc., Agoura Hills, California 91301

INTRODUCTION

Volatile organic compounds (VOCs) are emitted from manufacturing the multitude of consumer products used every day. In most manufacturing processes, either for the raw materials, intermediates, or the finished product, VOC-containing materials are present as chemicals, solvents, release agents, coatings, and decomposition products that eventually must be disposed. In manufacturing, there is usually a gaseous effluent that contains low concentrations of organics and is vented into the atmosphere. Chlorinated VOCs are some of the most common solvents used, and are now found in hazardous concentrations at many industrial and government installations. Cost effective technologies for disposal of VOCs are therefore being sought by government and by industry, and there is a need for reliable data concerning the decomposition mechanisms associated with these compounds. Non-thermal plasma methods using electrical discharges and electron beams are some of the emerging technologies for the disposal of these toxic substances. The electron beam method has been applied to the removal of vinyl chloride [1], trichloroethylene [2-3], carbon tetrachloride [4-6] and other types of volatile hydrocarbons from industrial off-gases [7]. Some of the electrical discharge reactors that have been investigated for VOC abatement include the pulsed corona [8-10], ferroelectric packed bed [9-10] dielectric-barrier discharge [11-17], surface discharge [18-19], gliding arc [20-21] and microwave [22].

There are many types of non-thermal plasma techniques that are being investigated for VOC abatement applications. The basic principle that these techniques have in common is to produce a plasma in which a majority of the electrical energy goes into the production of energetic electrons, rather than into gas heating. Through electron-impact dissociation and ionization of the background gas molecules, the energetic electrons produce free radicals and electron-ion pairs that, in turn, decompose the VOC molecules. Whatever the type of reactor, the plasma can induce three basic types of reactions with the VOC molecules, as shown in Fig. 1. Electron-impact dissociation of oxygen molecules produces O (and OH radicals in the presence of water vapor) that could oxidize the VOC molecules. Electron-impact ionization of the background air molecules produces electron-ion pairs. The electrons could decompose the VOC molecules via dissociative electron attachment.

The ions could decompose the VOC molecules via dissociative charge exchange. The decomposition pathway for a particular VOC depends on the reaction rate constants and the amount of radicals and electron-ion pairs produced in the plasma.

Radical-induced decomposition
$$e + O_2 \rightarrow e + O(^3P) + O(^1D)$$
$$O(^3P) + CCl_4 \rightarrow ClO + CCl_3$$
$$O(^1D) + H_2O \rightarrow OH + OH$$
$$OH + CCl_4 \rightarrow HOCl + CCl_3$$

Electron-induced decomposition
$$e + N_2 \rightarrow e + e + N_2^+$$
$$e + O_2 \rightarrow e + e + O_2^+$$
$$e + CCl_4 \rightarrow CCl_3 + Cl^-$$

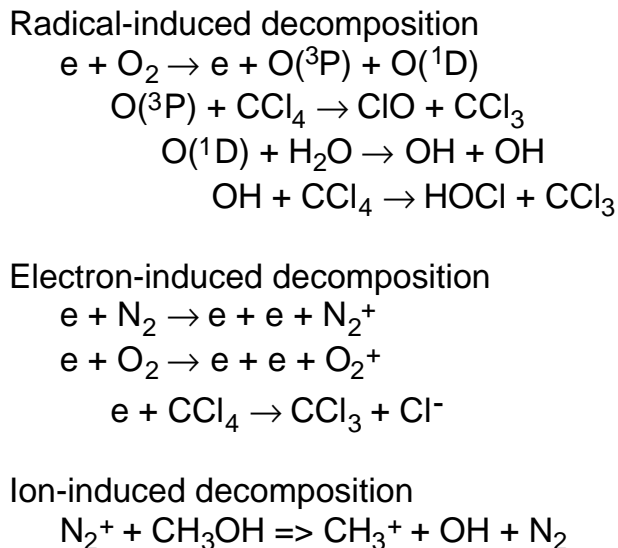Ion-induced decomposition
$$N_2^+ + CH_3OH => CH_3^+ + OH + N_2$$

Fig. 1. There are three basic types of chemical reactions responsible for the decomposition of volatile organic compounds: (a) decomposition via oxidation by O and OH free radicals or reduction by N atoms, (b) electron-induced decomposition via dissociative electron attachment, and (c) ion-induced decomposition via dissociative charge exchange.

The electron mean energy in a plasma reactor is very important because it determines the types of radicals produced in the plasma and the input electrical energy required to produce those radicals. Fig. 2 shows the dissipation of the input electrical power in a dry air discharge. Note that at low electron mean energies (< 5 eV) a large fraction of the input electrical energy is consumed in the vibrational excitation of N_2. Electron mean energies around 5 eV are optimum for the electron-impact dissociation of O_2, which is important for the production of O radicals. High electron mean energies are required to efficiently implement the dissociation of N_2. For VOCs that take advantage of electron-induced or ion-induced decomposition, high electron mean energies are required to efficiently implement the ionization of the background gas.

In terms of the electron energy distribution in the plasma, there are basically only two types of non-thermal atmospheric-pressure plasma reactors: electrical discharge reactors and electron beam reactors. Electrical discharge techniques can be implemented in many ways, depending on the electrode configuration and electrical power supply (pulsed, AC or DC). Two of the more extensively investigated types of electrical discharge reactors are the pulsed corona and the dielectric-barrier discharge, shown in Fig. 3. In the pulsed corona method, the reactor is driven by very short pulses of high voltage, thus creating short-lived discharge plasmas that consist of energetic electrons, which in turn produce the radicals responsible for the decomposition of the undesirable molecules. In a dielectric barrier discharge reactor, one or both of the electrodes are covered with a thin dielectric

layer, such as glass or alumina. Dielectric-barrier discharge reactors, also referred to as silent discharge reactors, are now routinely used to produce commercial quantities of ozone. Whereas in the pulsed corona method the transient behavior of the plasma is controlled by the applied voltage pulse, the plasma that takes place in a dielectric-barrier discharge self-extinguishes when charge build-up on the dielectric layer reduces the local electric field.
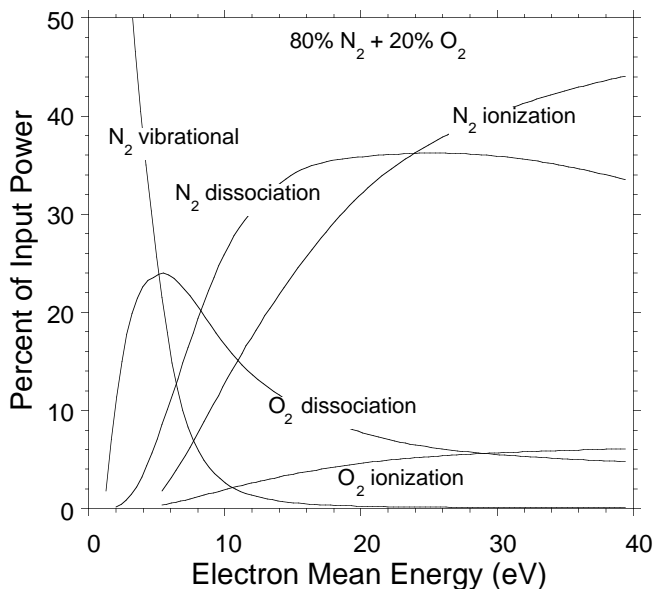

Fig. 2. Power dissipation in a dry air discharge, showing the percent of input power consumed in the electron-impact processes leading to vibrational excitation, dissociation and ionization of N_2 and O_2.
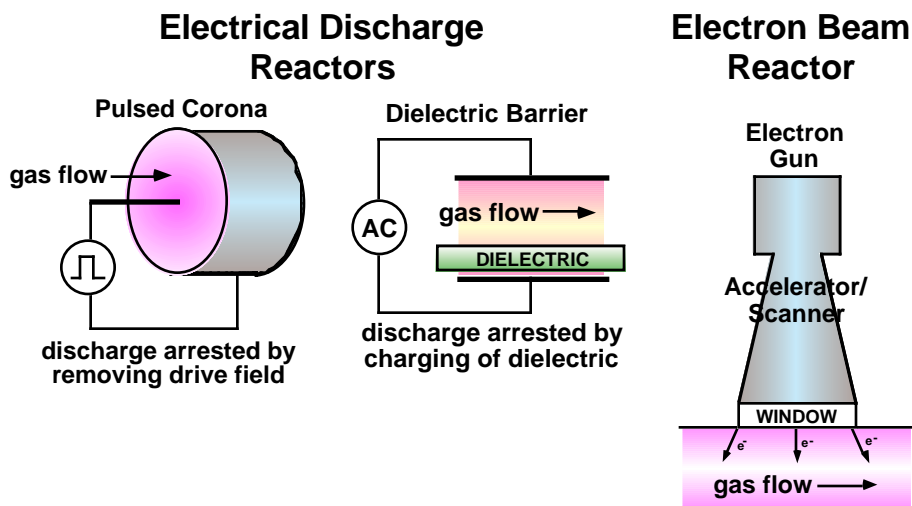

Fig. 3. There are basically two types of non-thermal atmospheric-pressure plasma reactors: electrical discharge reactors and electron beam reactors.

In this paper we present data on the non-thermal plasma processing of two representative VOCs: carbon tetrachloride and methanol. The investigation used a compact electron beam reactor, and two types of discharge reactors: a pulsed corona and a dielectric-barrier discharge. To the knowledge of the authors, this is the first comparison of the energy efficiency of electron beam, pulsed corona and dielectric-barrier discharge processing of these VOCs under identical gas conditions. For most electrical discharge reactors our analysis suggests that the attainable electron mean energy is rather limited and cannot be significantly enhanced by changing the electrode configuration or voltage waveform. Our experimental data confirms that there is no significant difference in the performance of our pulsed corona and dielectric-barrier discharge reactors. We observe that electron beam processing is remarkably more energy efficient than electrical discharge processing in decomposing either of these VOC molecules. During electron beam processing, the specific energy consumption is consistent with the energy required for the ionization of the background air molecules. For carbon tetrachloride, the dominant decomposition pathway is dissociative electron attachment. For methanol, the dominant decomposition pathway is dissociative charge exchange.

TEST FACILITY

All of our experiments were performed in a flow-through configuration. To characterize the energy consumption of the process for each VOC, the composition of the effluent gas was recorded as a function of the input energy density. The input energy density, Joules per standard liter, is the ratio of the power (deposited into the gas) to gas flow rate at standard conditions (25°C and 1 atm). The amount of VOC was quantified an FTIR analyzer and a gas chromatograph/mass spectrometer.

Our electron beam reactor used a cylindrical electron gun designed to deliver a cylindrically symmetric electron beam that is projected radially inward through a 5 cm wide annular window into a 17 cm diameter flow duct. An electron beam of 125 keV energy was introduced into the reaction chamber through a 0.7 mil thick titanium window. The electron beam current was produced from a low-pressure helium plasma in an annular vacuum chamber surrounding the flow duct.

Our pulsed corona reactor is a 1.5 mm diameter wire in a 60 mm diameter metal tube 300 mm long. The power supply is a magnetic pulse compression system capable of delivering up to 15-35 kV output into 100 ns FWHM pulses at repetition rates from 15 Hz to 1.5 kHz. The power input to the processor was varied by changing either the pulse energy or pulse repetition frequency. For the same energy density input, either method produced almost identical results. The gas mixtures were set with mass flow controllers. The gas and processor temperatures can be maintained at a temperature that can be controlled from 25°C to 300°C.

The dielectric-barrier discharge electrode structure has a similar electrode structure except that it has a dielectric material on the inside surface of the outer tube electrode. It consists of a 1.5 mm diameter wire in a 290 mm long alumina tube with inner and outer diameters of 53 mm and 58 mm, respectively. The middle 170 mm of the dielectric tube has aluminum foil coating the outside to form the other electrode.

4

ELECTRON AND CHEMICAL KINETICS

To calculate the ion and radical production yields by electrical discharge processing, we used the Boltzmann code ELENDIF [23] to calculate electron energy deposition. ELENDIF uses as input the specified gas composition and the electron-molecule collision cross sections. To calculate the ion and radical production yields by electron beam processing, we used the code DEGRAD [24]. DEGRAD also uses as input the specified gas composition and the electron-molecule collision cross sections. This code follows typical electrons as they perform successive collisions, and discrete energy bins are used to represent the energy degradation of an electron from a given beam energy. The procedure records the number of excitations, dissociations and ionizations, and the total number of all orders of secondary electrons. The chemical kinetics describing the subsequent interaction of the ions and radicals with the exhaust gas was studied using CHEMKIN-II [25].

RESULTS

In discharge processing, the rate coefficients for electron-impact dissociation and ionization reactions strongly depend on the electron mean energy in the discharge plasma. In pulsed corona and dielectric-barrier discharge reactors, the non-thermal plasma is produced through the formation of statistically distributed microdischarges. The electrons dissociate and ionize the background gas molecules within nanoseconds in the narrow channel formed by each microdischarge. The electron energy distribution in the plasma is complicated because the electric field is strongly non-uniform (e.g. because of strong space-charge field effects) and time dependent. However, most of the species responsible for the chemical processing are generated in the microdischarge channels already established during the main current flow. In each microdischarge column, the electrons acquire a drift velocity, v_d, and an average energy corresponding to an effective E/n, i.e., the value of the electric field E divided by the total gas density n. The efficiency for a particular electron-impact process can be expressed in terms of the G-value (number of dissociation or ionization reactions per 100 eV of input energy) defined as

$$G\text{-value} = 100 \, k / (v_d \, E/n)$$

where k is the rate coefficient (cm^3/molec-s). The rate coefficient k represents the number of reactions in a unit volume per unit time. The quantity $v_d \, E/n$ represents the amount of energy expended by the electrons in a unit volume per unit time. In Fig. 4 the calculated G-values for various electron-impact dissociation and ionization processes in dry air are shown as functions of the electron mean energy in the discharge plasma.

Under most conditions encountered in pulsed corona or dielectric-barrier discharge processing, the effective E/n is close to the value for breakdown (Paschen field) [26-27]. For dry air, the effective E/n is around 130 Td (1 Td = 10^{-17} V-cm^2), which corresponds to an electron mean energy of about 4 eV. This analysis suggests that the attainable electron mean energy is rather limited and cannot be significantly enhanced by changing the electrode configuration or voltage pulse parameters. Fig. 5 shows the comparison between pulsed corona and dielectric-barrier discharge processing of methanol in dry air at 120°C.

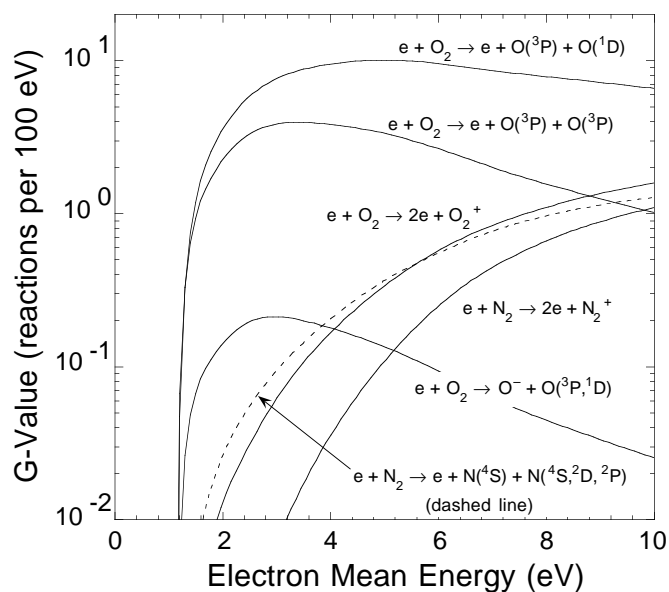Fig. 4. Calculated G-values (number of reactions per 100 eV of input energy) for dissociation and ionization processes in dry air, shown as functions of the electron mean energy in a discharge plasma.
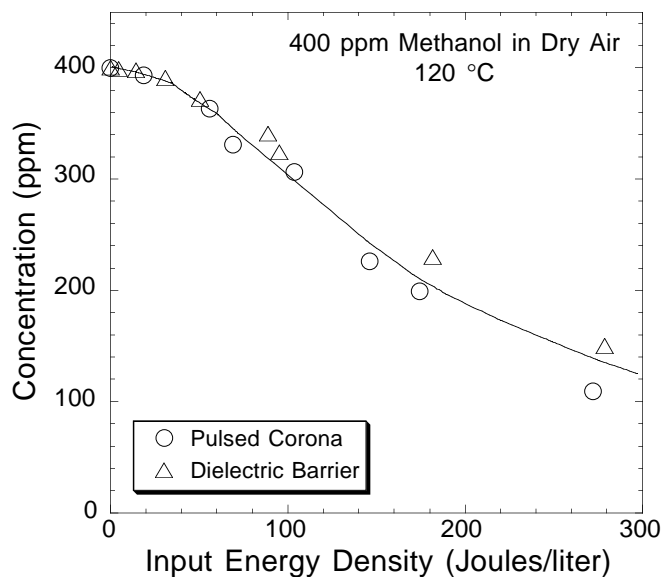

Fig. 5. Pulsed corona and dielectric-barrier discharge processing of 400 ppm methanol in dry air at 120°C. There is no significant difference in the performance of different types of electrical discharge reactors.

Our experimental data confirms that there is no significant difference in the performance of pulsed corona and dielectric-barrier discharge reactors.

In electron beam processing, the efficiency for a particular electron-impact process can be expressed in terms of the G-value, which is defined in the code DEGRAD as

$$\text{G-value} = 100 \; N_j \, / \, E_p$$

where N_j is the number of dissociation or ionization events, and E_p is the primary electron energy.

Table 1 shows a comparison of the calculated G-values for dissociation processes in dry air using an electron beam and a discharge reactor. Discharge plasma conditions are optimum for the dissociation of O_2. The production of O radicals is higher in a pulsed corona reactor compared to that in an electron beam reactor. Table 2 shows a comparison of the calculated G-values for ionization processes in dry air using an electron beam and a discharge reactor. The efficiency for production of electron-ion pairs is much higher in an electron beam reactor compared to that in a pulsed corona reactor.

Table 1. Calculated G-values (number of reactions per 100 eV of input energy) for dissociation processes in dry air using an electron beam and an electrical discharge reactor.

REACTION	Electron Beam	Discharge
$e + N_2 \rightarrow e + N(^4S) + N(^4S, ^2D, ^2P)$	1.2	0.17
$e + O_2 \rightarrow e + O(^3P) + O(^3P)$	1.3	4.0
$e + O_2 \rightarrow e + O(^3P) + O(^1D)$	2.65	10.0
$e + O_2 \rightarrow O^- + O(^3P, \, ^1D)$	0.11	0.19

Table 2. Calculated G-values (number of reactions per 100 eV of input energy) for ionization processes in dry air using an electron beam and an electrical discharge reactor.

REACTION	Electron Beam	Discharge
$e + N_2 \rightarrow 2e + N(^4S, \, ^2D) + N^+$	0.69	$< 10^{-6}$
$e + N_2 \rightarrow 2e + N_2^+$	2.27	0.044
$e + O_2 \rightarrow 2e + O_2^+$	2.07	0.17
$e + O_2 \rightarrow 2e + O(^1D) + O^+$	1.23	0.0016

In non-thermal plasma processing of a mixture containing very dilute concentrations of VOC molecules, the input electrical energy is dissipated by the primary electrons mostly in interactions with the background gas molecules. The energetic primary electrons produce free radicals and electron-ion pairs through electron-impact dissociation and ionization. In a

dry air mixture, electron-impact dissociation of molecular oxygen produces the ground state atomic oxygen $O(^3P)$ and excited atomic oxygen $O(^1D)$:

$$e + O_2 \rightarrow e + O(^3P) + O(^3P) \qquad (1a)$$

$$e + O_2 \rightarrow e + O(^3P) + O(^1D) \qquad (1b)$$

In addition, with energetic electrons, $O(^3P)$ and $O(^1D)$ can be produced via two-body dissociative attachment:

$$e + O_2 \rightarrow O^- + O(^3P,^1D) \qquad (1c)$$

As seen in Fig. 4 the main contribution to O radical production comes from the dissociation reactions (1a) and (1b).

The O radicals can dissociate CCl_4 into ClO and CCl_3 [28-30]:

$$O(^3P) + CCl_4 \rightarrow ClO + CCl_3 \qquad (3a)$$

$$O(^1D) + CCl_4 \rightarrow ClO + CCl_3 \qquad (3b)$$

Another mechanism for the dissociation of CCl_4 is through the secondary electrons. Electron-ion pairs are produced through various electron-impact ionization processes [31-32]:

$$e + N_2 \rightarrow 2e + N_2^+ \qquad (4)$$

$$e + N_2 \rightarrow 2e + N(^4S) + N^+ \qquad (5)$$

$$e + N_2 \rightarrow 2e + N(^2D) + N^+ \qquad (6)$$

$$e + O_2 \rightarrow 2e + O_2^+ \qquad (7)$$

$$e + O_2 \rightarrow 2e + O(^1D) + O^+ \qquad (8)$$

The secondary electrons can dissociate CCl_4 via dissociative electron attachment [17,18] to produce CCl_3 and a negative ion Cl^-:

$$e + CCl_4 \rightarrow CCl_3 + Cl^- \qquad (9)$$

The rate coefficient for reaction (9) is on the order of 10^{-7} cm^3/(molec-s) [33-34]. The rate coefficient for reaction (3a) is less than 10^{-14} cm^3/(molec-s) [28], while that for reaction (3b) is around 10^{-10} cm^3/(molec-s) [29-30]. An examination of the G-values shown in Tables 1 and 2 indicates that dissociative electron attachment will dominate the initial decomposition of CCl_4 for both electron beam and electrical discharge reactor conditions.

The charge exchange reaction of positive ions, such as N_2^+, with the background O_2 is fast, resulting in mostly O_2^+ ions [35]:

$$N_2^+ + O_2 \rightarrow N_2 + O_2^+ \qquad (10)$$

The positive ions react with Cl⁻ through the ion-ion neutralization reaction to produce Cl and O radicals:

$$Cl^- + O_2^+ \rightarrow Cl + 2O \tag{11}$$

In the absence of scavenging reactions for CCl_3, the input energy would be wasted because Cl and CCl_3 would simply recombine quickly to reform the original pollutant [36-37]:

$$Cl + CCl_3 + M \rightarrow CCl_4 + M \tag{12}$$

Fortunately, the presence of O_2 scavenges the CCl_3 through the fast reaction [38-39]:

$$CCl_3 + O_2 + M \rightarrow CCl_3O_2 + M \tag{13}$$

The CCl_3O_2 species undergoes a chain reaction involving the Cl radical and produces phosgene ($COCl_2$) as one of the main organic products [30,40]:

$$Cl + CCl_3O_2 \rightarrow CCl_3O + ClO \tag{14}$$

$$CCl_3O \rightarrow COCl_2 + Cl \tag{15}$$

The ClO species produces additional Cl radicals through a reaction with the O radicals [30,41]:

$$O + ClO \rightarrow Cl + O_2 \tag{16}$$

The other major product is Cl_2 which is formed by the reaction [41]:

$$Cl + Cl + M \rightarrow Cl_2 + M \tag{17}$$

The CCl_3 species from reaction (9) can also be scavenged by O [42]:

$$CCl_3 + O \rightarrow COCl_2 + Cl \tag{18}$$

and by N [43]:

$$CCl_3 + N \rightarrow ClCN + 2Cl \tag{19}$$
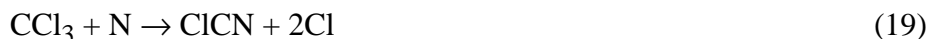
The apparent two-body rate constant for scavenging reaction (13) is 1.4×10^{-9} $T^{-1.1}$ (cm^3/molec-s). The rate constants are 4.2×10^{-11} and 1.7×10^{-11} (cm^3/molec-s) for scavenging reactions (18) and (19), respectively. Because of the much larger density of O_2 compared to O or N, the scavenging of CCl_3 by reactions (18) and (19) are therefore negligible compared to reaction (13) during processing in dry air.

Fig. 6 shows the results of experiments on electron beam and pulsed corona processing of 100 ppm of CCl_4 in dry air (20% O_2 80% N_2) at 25°C. The pulsed corona reactor requires 1277 Joules/liter for 90% decomposition of CCl_4, whereas the electron beam reactor requires only 20 Joules/liter to achieve the same level of decomposition.

An analysis of the rates of the reactions discussed above suggests that the rate limiting step in the decomposition of CCl_4 is determined by the dissociative attachment of CCl_4 to the thermalized electrons in the created plasma. The specific energy consumption for CCl_4 removal is therefore determined by the specific energy consumption (or G-value) for creating electron-ion pairs. Table 2 shows the calculated G-values for the ionization

processes (4)-(8). For electron beam processing of dry air, the ionization G-value corresponds to a specific energy consumption of 33 eV per electron-ion pair produced. For pulsed corona processing, we calculate a specific energy consumption of around 1400 eV per electron-ion pair, assuming an effective electron mean energy of 4 eV in the discharge plasma. To first order, the calculated specific energy consumption for electron-ion pair production agrees very well with our experimentally observed specific energy consumption for CCl_4 decomposition. The results shown in Fig. 6 demonstrate that for VOCs requiring copious amounts of electrons for decomposition, electron beam processing is much more energy efficient than electrical discharge processing.
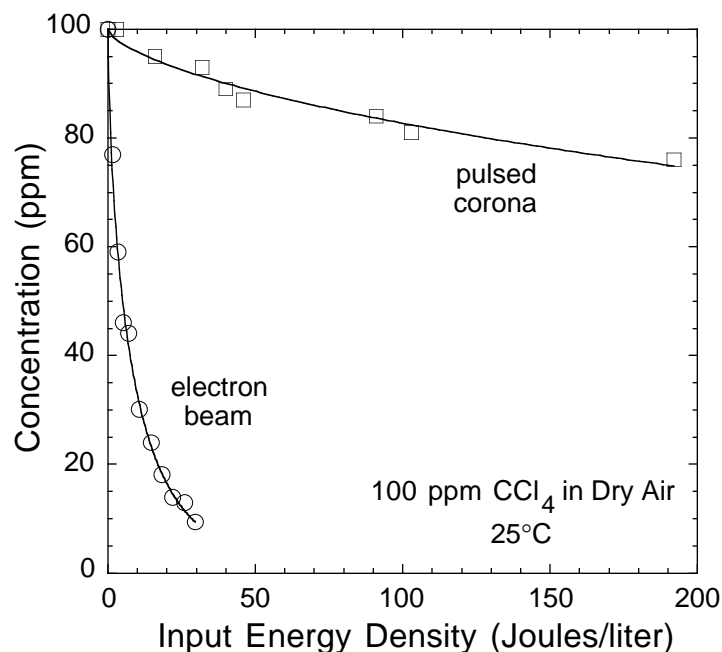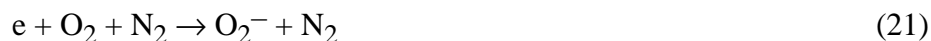

Fig. 6. Comparison between electron beam and pulsed corona processing of 100 ppm of carbon tetrachloride in dry air at 25°C.

After the concentration of CCl_4 has decreased to a few tens of ppm, the three-body attachment of thermal electrons to oxygen molecules [44]:

$$e + O_2 + O_2 \rightarrow O_2^- + O_2 \tag{20}$$

$$e + O_2 + N_2 \rightarrow O_2^- + N_2 \tag{21}$$

becomes a significant electron loss pathway compared to reaction (9). The rate constants for reactions (20) and (21) are $k_{(20)} = 2.5 \times 10^{-30}$ and $k_{(21)} = 0.16 \times 10^{-30}$ cm^6/s, respectively. The attachment frequency of thermal electrons to O_2 in dry air at atmospheric pressure is thus

$$\nu_{O2} = k_{(20)} [O_2]^2 + k_{(21)} [N_2] [O_2] \approx 0.8 \times 10^8 \text{ s}^{-1}.$$

10

The attachment rate coefficient for thermal electrons to CCl_4 is $k_{(9)} = 4 \times 10^{-7}$ cm^3/s. For 100 ppm CCl_4, the attachment frequency to CCl_4 is thus

$$\nu_{CCl4} = k_{(9)} [CCl_4] \approx 10^9 \text{ s}^{-1}.$$

When the concentration of CCl_4 is down to around 10 ppm, the electrons will attach to oxygen molecules as frequently as to CCl_4 molecules.

Although the dominant pathway (dissociative electron attachment) for the initial decomposition of CCl_4 is the same in electron beam and pulsed corona processing, the composition of the final products are not the same. In pulsed corona processing, a larger amount of O radicals is produced relative to the amount of electrons. Even though these O radicals contribute only a small fraction to the initial decomposition of CCl_4, they do interact significantly with phosgene to change the composition of the final products [28,45]:

$$O + COCl_2 \rightarrow ClO + COCl \qquad\qquad (22)$$

$$COCl + M \rightarrow CO + Cl + M \qquad\qquad (23)$$

$$O + COCl \rightarrow CO_2 + Cl \qquad\qquad (24)$$

Our model for the decomposition mechanism predicts a difference in product yields between electron beam and pulsed corona processing at the minimum energy required for near complete decomposition of CCl_4. For around 95% decomposition of 100 ppm CCl_4 in dry air by electron beam processing, the final products consist of around 100 ppm Cl_2 and 100 ppm $COCl_2$. For the same level decomposition of 100 ppm CCl_4 in dry air by pulsed corona processing, the final products consist of around 160 ppm Cl_2, 40 ppm $COCl_2$, 50 ppm CO and 10 ppm CO_2. Of course, with excessive energy deposition all the $COCl_2$ would eventually be converted into CO_x and Cl_2. However, as noted in References [46] and [47], the Cl_2 and $COCl_2$ products can be easily removed from the gas stream; e.g. they dissolve and/or dissociate in aqueous solutions and combine with $NaHCO_3$ in a scrubber solution to form NaCl [47].

Fig. 7 shows the results of experiments on electron beam and pulsed corona processing of 100 ppm of methanol in dry air at 25°C. The pulsed corona reactor requires 450 Joules/liter for 90% decomposition of methanol, whereas the electron beam reactor requires only around 15 Joules/liter to achieve the same level of decomposition. In this case, the electron beam method is more efficient because the decomposition proceeds mainly via a dissociative charge exchange reaction

$$N_2^+ + CH_3OH \rightarrow CH_3^+ + OH + N_2 \qquad\qquad (25)$$
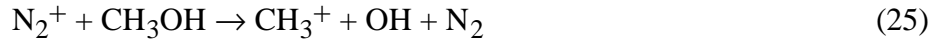
The OH radicals resulting from the initial decomposition reaction (25) in turn may lead to additional decomposition of methanol via $OH + CH_3OH$.

To verify that the primary decomposition during electron beam processing does not proceed through an oxidation pathway using O radicals, we performed the experiment using N_2 as the background gas. As shown in Fig. 8, the specific energy consumption in dry air is almost identical to that in N_2.
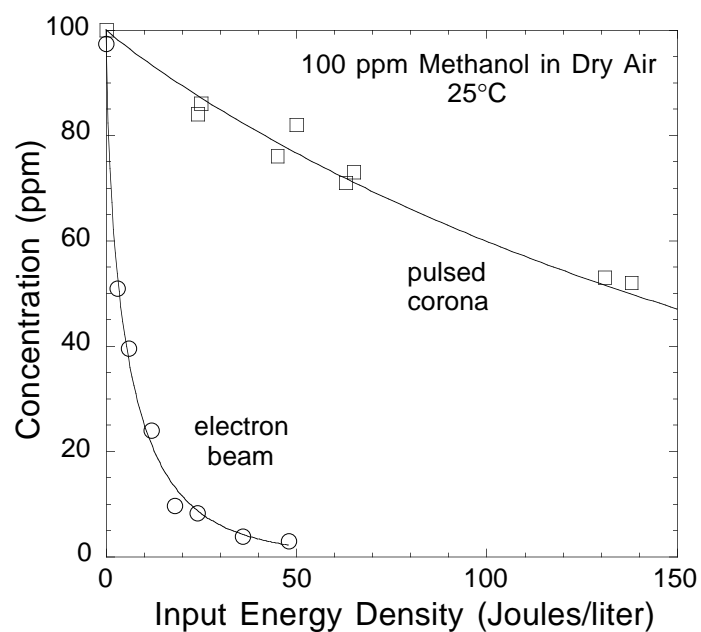
Fig. 7. Comparison between electron beam and pulsed corona processing of 100 ppm of methanol in dry air at 25°C.
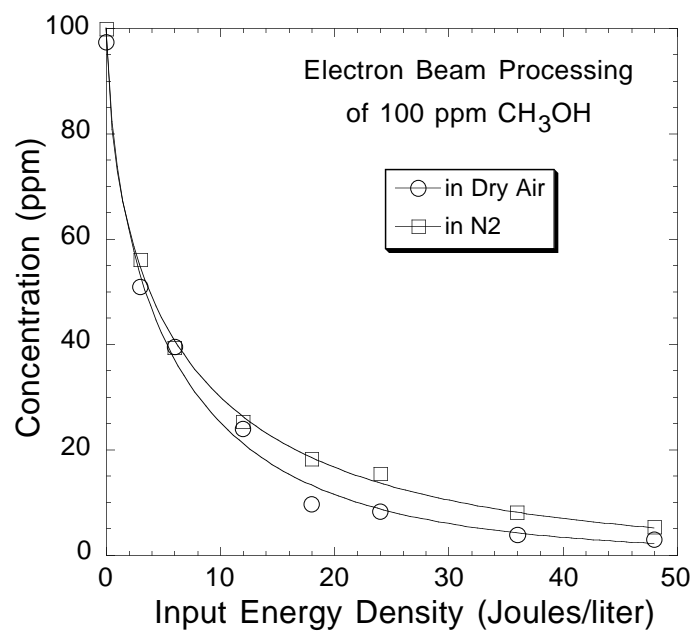

Fig. 8. Comparison between electron beam of 100 ppm of methanol in dry air and electron beam processing of 100 ppm of methanol in N_2. Gas temperature is 25°C.

REFERENCES

[1] R. C. Slater and D. H. Douglas-Hamilton, *J. Appl. Phys.* **52**, 5820 (1981).

[2] H. Scheytt, H. Esrom, L. Prager, R. Mehnert, and C. von Sonntag, in *Non-Thermal Plasma Techniques for Pollution Control: Part B - Electron Beam and Electrical Discharge Processing*, edited by B. M. Penetrante and S. E. Schultheis (Springer-Verlag, Heidelberg, 1993) pp. 91-102.

[3] S. M. Matthews, A. J. Boegel, J. A. Loftis, R. A. Caufield, B. J. Mincher, D. H. Meikrantz, and R. J. Murphy, *Radiat. Phys. Chem.* **42**, 689 (1993).

[4] L. Bromberg, D. R. Cohn, M. Kock, R. M. Patrick, and P. Thomas, *Phys. Lett. A* **173**, 293 (1993).

[5] M. Koch, D. R. Cohn, R. M. Patrick, M. P. Schuetze, L. Bromberg, D. Reilly and P. Thomas, *Phys. Lett. A* **184**, 109 (1993).

[6] B. M. Penetrante, M. C. Hsiao, B. T. Merritt, G. E. Vogtlin, P. H. Wallman, A. Kuthi, C. P. Burkhart and J. R. Bayless, *Phys. Lett. A* (in press, 1996).

[7] H.-R. Paur, in *Non-Thermal Plasma Techniques for Pollution Control: Part B - Electron Beam and Electrical Discharge Processing*, edited by B. M. Penetrante and S. E. Schultheis (Springer-Verlag, Heidelberg, 1993) pp. 77-90.

[8] M. C. Hsiao, B. T. Merritt, B. M. Penetrante, G. E. Vogtlin, and P. H. Wallman, *J. Appl. Phys.* **78,** 3451 (1995).

[9] T. Yamamoto, K. Ramanathan, P. A. Lawless, D. S. Ensor, J. R. Newsome, N. Plaks, G. H. Ramsey, C. A. Vogel, and L. Hamel, *IEEE Trans. on Ind. Appl.* **28**, 528 (1992).

[10] T. Yamamoto, P. A. Lawless, M. K. Owen, D. S. Ensor, and C. Boss, in *Non-Thermal Plasma Techniques for Pollution Control: Part B - Electron Beam and Electrical Discharge Processing*, edited by B. M. Penetrante and S. E. Schultheis (Springer-Verlag, Heidelberg, 1993) pp. 223-238.

[11] D. Evans, L. A. Rosocha, G. K. Anderson, J. J. Coogan, and M. J. Kushner, *J. Appl. Phys.* **74**, 5378 (1993).

[12] L. A. Rosocha, G. K. Anderson, L. A. Bechtold, J. J. Coogan, H. G. Heck, M. Kang, W. H. McCulla, R. A. Tennant, and P. J. Wantuck, in *Non-Thermal Plasma Techniques for Pollution Control: Part B - Electron Beam and Electrical Discharge Processing*, edited by B. M. Penetrante and S. E. Schultheis (Springer-

Verlag, Heidelberg, 1993) pp. 281-308.

[13] W. C. Neely, E. I. Newhouse, E. J. Clothiaux, and C. A. Gross, in *Non-Thermal Plasma Techniques for Pollution Control: Part B -Electron Beam and Electrical Discharge Processing*, edited by B. M. Penetrante and S. E. Schultheis (Springer-Verlag, Heidelberg, 1993) pp. 309-320.

[14] E. I. Newhouse, W. C. Neely, E. J. Clothiaux, and J. W. Rogers, in *ACS Symposium on Emerging Technologies in Hazardous Waste Management VI*, pp. 207-210.

[15] E. J. Clothiaux, J. A. Koropchak, and R. R. Moore, *Plasma Chem. Plasma Process.* **4**, 15 (1984).

[16] M. E. Fraser, D. A. Fee, and R. S. Sheinson, *Plasma Chem. Plasma Process.* **5**, 163 (1985).

[17] M. E. Fraser and R. S. Sheinson, *Plasma Chem. Plasma Process.* **6**, 27 (1986).

[18] S. Masuda, in *Non-Thermal Plasma Techniques for Pollution Control: Part B - Electron Beam and Electrical Discharge Processing*, edited by B. M. Penetrante and S. E. Schultheis (Springer-Verlag, Heidelberg, 1993) pp. 199-210.

[19] T. Oda, T. Takahashi, H. Nakano, and S. Masuda, in *Proceedings of the 1991 IEEE Industrial Application Society Meeting* (Dearborn, MI, September/October 1991) pp. 734-739.

[20] A. Czernichowski and H. Lesueur, in *Proceedings of the 10th International Symposium on Plasma Chemistry* (Bochum, Germany, 1991).

[21] A. Czernichowski and T. Czech, in *Proceedings of the 3rd International Symposium on High-Pressure Low-Temperature Plasma Chemistry* (Strasbourg, France, 1991).

[22] L. J. Bailin, M. E. Sibert, L. A. Jonas, and A. T. Bell, *Environ. Sci. Tech.* **9**, 254 (1975).

[23] W. L. Morgan and B. M. Penetrante, *Comp. Phys. Comm.* **58**, 127-152 (1990).

[24] B. M. Penetrante and J. N. Bardsley, *J. Appl. Phys.* **66**, 1871-1874 (1989).

[25] R. J. Kee, F. M. Rupley and J. A. Miller, "Chemkin-II: A FORTRAN Chemical Kinetics Package for the Analysis of Gas Phase Chemical Kinetics," Sandia National Laboratories Report No. SAND89-8009B UC-706 (April 1992).

[26] B. Eliasson and U. Kogelschatz, *J. Phys. B: At. Mol. Phys.* **19**, 1241 (1986).

[27] B. M. Penetrante, in *Non-Thermal Plasma Techniques for Pollution Control - Part A: Overview, Fundamentals and Supporting Technologies*, B. M. Penetrante and S. E. Schultheis, Eds. (Springer-Verlag, Berlin Heidelberg, 1993) pp. 65-90.

[28] J. T. Herron, *J. Phys. Chem. Ref. Data* **17**, 967 (1988).

[29] J. A. Davidson, H. I. Schiff, T. J. Brown, C. J. Howard, *J. Chem. Phys.* **69**, 4277 (1978).

[30] R. Atkinson, D. L. Baulch, R. A. Cox, R. F. Hampson, Jr., J. A. Kerr, J. Troe, *J. Phys. Chem. Ref. Data* **21**, 1125-1568 (1992).

[31] Y. Itikawa, M. Hayashi, A. Ichimura, K. Onda, D. Sakimoto, K. Takayanagi, M. Nakamura, H. Nishimura and T. Takayanagi, *J. Phys. Chem. Ref. Data* **15**, 985 (1986).

[32] Y. Itikawa, A. Ichimura, K. Ondaz, K. Sakimoto, K. Takayanagi, Y. Hatano, M. Hayashi, H. Nishimura and S. Tsurubuchi, , *J. Phys. Chem. Ref. Data* **18**, 23 (1989).

[33] A. A. Christodoulides and L. G. Christophorou, *J. Chem. Phys.* **54**, 4691 (1971).

[34] J. A. Ayala, W. E. Wentworth and E. C. M. Chen, *J. Phys. Chem.* **85**, 3989 (1981).

[35] D. L. Albritton, *Atom. Data Nucl. Data Tables* **22**, 1 (1978).

[36] F. Danis, F. Caralp, B. Veyret, H. Loirat, R. Lesclaux, *Int. J. Chem. Kinet.* **21**, 715 (1989).

[37] T. Ellermann, *Chem. Phys. Lett.* **189**, 175 (1992).

[38] F. Danis, F. Caralp, M. T. Rayez, R. Lesclaux, *J. Phys. Chem.* **95**, 7300-7307 (1991).

[39] F. F. Fenter, P. D. Lightfoot, J. T. Niiranen, D. Gutman, *J. Phys. Chem.* **97**, 313-5320 (1993).

[40] J. J. Russell, J. A. Seetula, D. Gutman, F. Danis, F. Caralp, P. D. Lightfoot, R. Lesclaux, C. F. Melius, S. M. Senkan, *J. Phys. Chem.* **94**, 3277 (1990).

[41] D. L. Baulch, J. Duxbury, S. J. Grant, D. C. Montague, *J. Phys. Chem. Ref. Data* **10**, Suppl. 1,1-1 (1981).

[42] J. T. Herron, *J. Phys. Chem. Ref. Data* **17**, 967 (1988).

[43] S. C. Jeoung, K. Y. Choo and S. W. Benson, *J. Phys. Chem.* **95**, 7282 (1991).

[44] L. M. Chanin, A. V. Phelps and M. A. Biondi, *Phys. Rev.* **128**, 219 (1962).

[45] W.-D. Chang and S. M. Senkan, *Environ. Sci. Tech.* **23**, 442 (1989).

[46] D. Evans, L. A. Rosocha, G. K. Anderson, J. J. Coogan and M. J. Kushner, *J. Appl. Phys.* **74**, 5378 (1993).

[47] R. M. Patrick and K. Hadidi, An Electron Beam Plasma System for Halogenated Hydrocarbon Vapor Destruction, Preprint No. 95-WP77B.04, 88th Annual Meeting & Exhibition of the Air & Waste Management Association, San Antonio, TX (18-23 June 1995).